Density Functional Study of Tetra-Atomic Clusters and Complexes of the Group 16 Elements: Trends in Structure and Bonding

Galina Orlova[†] and John D. Goddard*

Department of Chemistry and Biochemistry, University of Guelph, Guelph, Ontario, Canada, N1G2W1

Received: March 10, 1999; In Final Form: June 24, 1999

Se_4 and Te_4 clusters, the intermolecular weakly bound charge-transfer complexes $(Se_2)(O_2)$ and $(Te_2)(O_2)$, and the $(X_2)(Y_2)$ and (XY)(YX) mixed compounds (X, Y = S, Se, Te) were studied using density functional theory with all-electron and effective core potential basis sets. All systems were analyzed in terms of interactions of the diatomic molecules. The energetically favorable "face to face" binding of the diatomic moieties leads to delocalization of the electron density in the high-lying occupied π^*-antibonding orbitals of the tetra-atomic products. The cis structures are minima for all systems considered as a result of this delocalization. For the clusters and mixed compounds, the cis tetra-atomic structures formed by the diatomic molecules with equal or similar electronegativities correspond to global minima. The diatomic fragments in these compounds are nonparallel and have shorter bond lengths than their free diatomic values. For the clusters, the other low-lying isomers ordered according to their relative stabilities are trans, branched ring, and puckered ring. The increase in the delocalization of bond lengths leads to a decrease in relative stabilities. The rectangular configuration was predicted to be a transition state in the degenerate interconversion of two cis forms of Se_4 with a chemically insignificant barrier. For Te_4, this barrier disappears and the geometry of the cis global mimima is extremely close to the rectangular structure. The stability of the (XY)(YX) compounds with heteronuclear diatomic fragments relative to the $(X_2)(Y_2)$ isomers with the homonuclear diatomic species increases with a decrease in the difference between the electronegativities of the X and Y atoms. The cis structures of $(Se_2)(O_2)$ and $(Te_2)(O_2)$ with the larger difference in electronegativities between the diatomic moieties correspond to local minima.

Introduction

The diatomic molecules S_2, Se_2, and Te_2 can be readily isolated in a solid argon matrix from superheated vapors. These X_2 molecules may be considered as the conceptual building blocks for the X_4 clusters which have been observed spectroscopically.[1a−d] These tetra-atomic compounds are known to be less stable than larger clusters of the chalcogens, but Se_4 rings are incorporated into infinite chains of amorphous selenium[1e] and exist in selenium gas. The use of selenium in the xerographic process has stimulated research on small selenium clusters.[1e,h] Dithio-, diselena-, and ditelluradiazolyl dimers contain S_4, Se_4, and Te_4 fragments and are important building blocks in the design of low-dimensional molecular conductors.[1f,11]

Experiments suggest at least two nearly degenerate isomers of the X_4 species, but it has proven impossible to extract information on the pure forms of these isomers. Thus, theory can be used profitably to examine the structures and relative energies of the X_4 isomers. Very extensive high-level ab initio investigations have been carried out on the S_4 potential energy surface.[2−5] It has been pointed out that at the multireference ab initio level two interacting triplet S_2 molecules can form four nearly isoenergetic S_4 isomers with closed-shell singlet electronic states as illustrated in Figure 1. The global minimum was predicted to have the open C_{2v} cis structure **I**. The C_{2h} trans isomer **III** is closest in energy to this C_{2v} form. A branched three-membered ring **IV** (C_s) and a four-membered puckered ring **V** (D_{2d}) lie higher in energy.

The X_4 species show similar vibrational spectra and thus it was proposed that all the tetra-atomic chalcogen clusters have similar potential energy surfaces. Andrews et al. using ab initio computations on S_4 as a guide for the other X_4 species assigned the IR bands of Se_4[1d] and Te_4[1c] to the C_{2v} cis isomers and to the C_s branched ring isomers. These results do not agree with earlier pioneering computations on the Se_4 cluster by Hohl et al.[6b] with parameter-free local density functional theory (LDFT) and molecular dynamics. To the best of our knowledge, theoretical investigations on Te_4 have not been reported.

Unlike the tetra-atomic chalcogens, no neutral O_4 structures in the ground electronic state were observed experimentally.[1g,i,j,7] O_2 can form tetra-atomic species in combination with the chalcogen diatomic molecules. Spectroscopic data[12] indicated weakly bound $(S_2)(O_2)$ and $(Se_2)(O_2)$ intermolecular complexes in a solid argon matrix with very similar IR spectra. The small blue shifts of 8 cm^{-1} for the X_2 subunits (X = S, Se) and the red shift of 148 cm^{-1} for the O_2 moiety[12] suggested the transfer of electron density from X_2 to the more electronegative O_2. For the $(S_2)(O_2)$ complex,[12] the BLYP functional predicted a C_{2v} cis minimum energy structure and binding energies of −3 to −5 kcal/mol. The predicted changes in harmonic vibrational frequencies were in good agreement with experiment. The possible formation of a $(Te_2)(O_2)$ complex has not been considered previously.

In addition to the clusters X_4 and the charge-transfer complexes $(X_2)(O_2)$, there exist intermediate cases of interaction when the two chalcogen diatomics have similar electronegativities: the $(Se_2)(S_2)$, $(Te_2)(S_2)$, and $(Te_2)(Se_2)$ systems. These

[†] Permanent address: Institute of Physical and Organic Chemistry, Rostov University, Rostov-on-Don, 344090, Russian Federation.

10.1021/jp990848d CCC: $18.00
Published on Web 07/30/1999

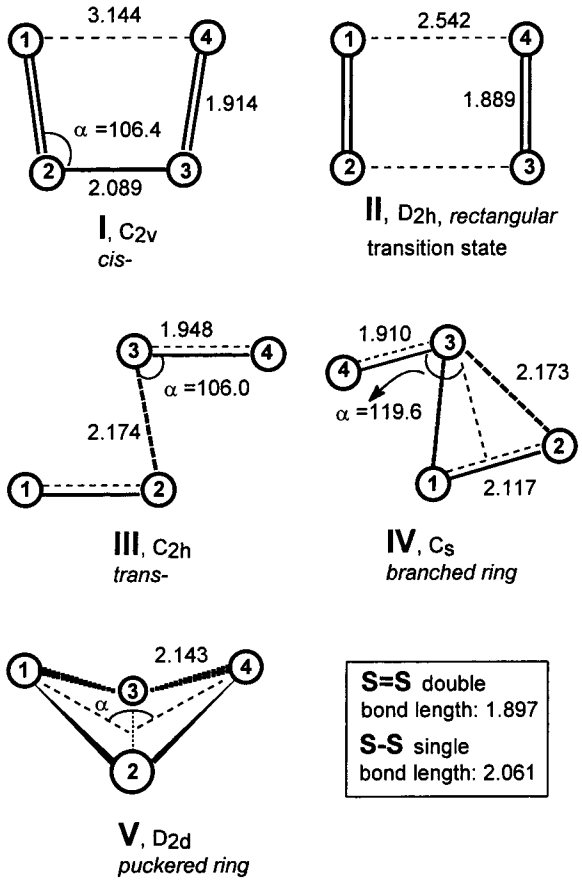

Figure 1. Structures of the S_4 clusters **I**−**V** along with selected geometrical parameters (in Å and deg) from ref 2. All values were computed with CISD/DZP. The standard S−S single bond length corresponds to the experimental value for the HSSH molecule.

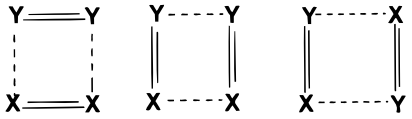

Figure 2. Possible structures of the mixed X_2Y_2 compounds.

compounds could be analyzed in terms of the interactions of triplet state SeS, SeTe, and TeS heteronuclear diatomic molecules which are known experimentally.[8a] Three types of mixed X_2Y_2 structures (X, Y are chalcogens) may be envisaged as depicted in Figure 2. Experimental studies of larger mixed Se_xS_y rings have been reported (see ref 29 and references therein). Se−Te crystals, amorphous films,[8b] and mixed chalcogen polycations[8d] are known experimentally. The chemistry of tellurium−sulfur complexes was discussed by Haiduc et al.[8c] Earlier theoretical investigations[29] of the seven- and eight-membered mixed Se_xS_y rings with LDFT predicted an energetic preference for the isomers with S−S or Se−Se linkages compared to isomers with Se−S bonds. Ziegler et al.[8e] studied several possible structures of $Te_4S_4^{n+}$ ions within the LDFT approximation.

We present here the first nonlocal DFT study of the structure and bonding in the X_4 (X = Se, Te) clusters, intermolecular $(X_2)(O_2)$ charge-transfer complexes, and the mixed complexes X_2Y_2 (X, Y═S, Se, Te). All systems were analyzed in terms of the interaction of diatomic fragments. Accurate theoretical studies of these systems already are known to present difficulties. An adequate description of the S_4 potential energy surface was obtained only with very high-level multireference methods.[2,4] In addition, the application of DFT to rather weakly bound intermolecular charge-transfer complexes approaches the limit of reliability of present techniques.[13]

Theoretical Details

All theoretical predictions were made with the GAUSSIAN98[14] package. Becke's 1988 (B)[15] functional with gradient correction of the density and Becke's three-parameter hybrid functional (B3),[16] which incorporates a contribution due to Hartree−Fock (HF) exchange, were used to model the exchange. Correlation was included via the functionals of Lee, Yang, and Parr (LYP)[17] with local and nonlocal terms. Thus, the exchange-correlation functionals used were BLYP and B3LYP.

The probable influence of the HF exchange component was considered before choosing between pure and hybrid DFT potentials. In the general case, the HF exchange component ameliorates the typical DFT overestimation of bond lengths and underestimation of energy gaps. However, the failure of the HF prediction of energetics for systems with strong electron correlation effects makes the hybrid DFT methods unsuitable for the quantitatively accurate description of the potential energy surface of such systems. For the clusters considered herein, the HF method overestimates the stability of the puckered ring structures very significantly.[2] Thus, the inclusion of HF exchange in the exchange-correlation potential (B3LYP has 20% HF exchange) would not be expected to produce the correct energetics. For the same reason the hybrid B3 failed to predict adequately the stability of the $(S_2)(O_2)$ complex.[12] Those authors[12] noted that the HF method (HF/TZ2P) itself predicts the $(S_2)(O_2)$ complex to be thermodynamically unstable by 111 kcal/mol above free S_2 and O_2. Therefore, a lack of stability of the $(S_2)(O_2)$ complex with the B3 functional could be anticipated. To demonstrate the influence of the HF exchange component on the energetics of the X_4 species, we made one series of predictions with B3LYP on the Te_4 cluster. The pure B-exchange functional was taken as the basic method for all other molecules considered herein.

It should be noted that in cases where both HF and pure DFT methods fail but with opposite signs for the errors, the inclusion of HF exchange may improve the energetic prediction from DFT. The Salahub group's[13] research with DFT on the charge-transfer complex between ethylene and Cl_2 has shown that the pure B-potential overestimates and HF underestimates the binding energy. The inclusion of the HF exchange component does improve the computed energetics. B3LYP yields a binding of −3.7 kcal/mol and the BH and H half-and-half functional with 50% HF exchange predicts −2.1 kcal/mol binding in good agreement with experiment. As a second example, the B3 functional predicted the correct relative stability of the D_{3h} rings compared to the C_{2v} open structures of the X_3 (X = O, S, Se) systems.[24] HF overestimated and the pure B-functional underestimated these energy differences.

DFT studies of those X_3 molecules[24] have shown that a change in the correlation functional plays a relatively minor role in predictions for these systems with strong nondynamical correlation. Thus, the influence of different correlation corrections was not examined herein and LYP was used throughout.

Several all-electron basis sets were employed. For predictions on the Se_4 and the $(Se_2)(O_2)$ species the valence triple-ζ (TZ) 6-311[18a] basis set was augmented with diffuse functions (+) and polarization functions 2df (two sets of d-type and one set of f-type polarization functions). The 6-31G(d),[18b] 6-311G(2df), 6-311+G(2df), and 6-311G(3df) basis sets were employed in initial computational tests on S_4. The large (18s14p8d) all-electron basis set of Huzinaga,[19] HD, was used for Te_4. Basis

TABLE 1: DFT Prediction of Bond Lengths *R* (Å), Harmonic Vibrational Frequencies ω (cm^{-1}), and Force Constants *f* (mDyne/Å) for Selected Group 16 Diatomic Molecules

method	*R*	ω	*f*	*R*	ω	*f*
		$^3\Sigma_g^-O_2$			$^3\Sigma_g^-S_2$	
UBLYP/						
6-311+g(2df)	1.229	1495	21.1	1.936	664	8.3
6-311g(2df)	1.230	1503	21.3	1.935	663	8.3
6-311g(3df)	1.228	1512	21.5	1.928	668	8.4
6-31g(BPF)				1.963	657	8.1
LanL2DZ(BPF)	1.247	1503	21.3	1.967	649	7.9
CEP-121g(BPF)				1.971	650	8.0
Cep-31g(BPF)	1.258	1504	21.3			
experiment	1.207[9d]	1580[a] 1552[9e b]		1.88[9c]	717[9b b]	
		$^3\Sigma_g^-Se_2$			$^3\Sigma^-SeS$	
UBLYP/						
6-311+g(2df)	2.220	354	5.9	2.081	509	5.9
LanL2DZ(BPF)	2.247	350	5.8	2.106	498	5.6
experiment	2.14[9c]	382[9a a]			556[8 b]	
		$^3\Sigma^-TeS$			$^3\Sigma^-SeTe$	
UBLYP/						
LanL2DZ(BPF)	2.292	427	4.0	2.429	288	4.0
experiment[8]		471[b]			314[b]	
		$^3\Sigma_g^-Te_2$				
UBLYP/						
Cep-31g(d)	2.698	211	3.4			
Cep-31g(BPF)	2.655	225	3.9			
LanL2DZ(BPF)	2.618	231	4.1			
HD	2.659	227	4.0			
UB3LYP/						
Cep-31g(d)	2.662	225	3.9			
experiment	2.54[9c]	246[1c b]				

[a] Fundamental values obtained in gas phase. [b] Fundamental values obtained in solid argon.

sets with pseudopotentials for the core electrons as incorporated in GAUSSIAN98 also were employed: the Stevens-Basch-Krauss effective core potential (ECP) triply split basis CEP-121,[20] split-valence CEP-31G,[20] and the Los Alamos ECP LanL2 with double-ζ (DZ) quality valence basis set.[21] These basis sets were augmented with one set of polarization functions (BPF) with the exponents recommended by Basch;[22] $\alpha_d(O) = 0.85$, $\alpha_d(S) = 0.49$, $\alpha_d(Se) = 0.32$, and $\alpha_d(Te) = 0.22$. The standard polarization function included in the GAUSSIAN98 code for Te with $\alpha_d(Te) = 0.532$ was used for comparison.

Table 1 presents DFT results on selected group 16 diatomic molecules with the various basis sets along with the available experimental data. These diatomic results are the reference data in our further analysis of the tetrameric species. The LanL2DZ basis augmented with the BPF yields reasonable results which agree well with the much more computationally expensive all electron 6-311+G(2df) results and with experiment. Thus, LanL2DZ(BPF) was the core potential and basis set of choice. The very computationally economic CEP-31G(BPF) sets were used for the tellurium compounds. Table 1 shows that, in general, DFT approaches with all basis sets systematically overestimate the bond lengths and underestimate the harmonic vibrational frequencies.

Binding energies (ΔE_{bind}) were calculated as the difference between the total energy of the tetra-atomic system and the sum of the total energies of two triplet diatomic molecules. Zero-point vibrational energy (ZPVE) corrections were omitted from the predicted relative energies and ΔE_{bind} in the clusters and the mixed compounds (Tables 3−5, Figures 8−10) since the changes in the energetics due to the ZPVE corrections are very small. ZPVE corrections were included in the predicted ΔE_{bind} for the weakly bound $(X_2)(O_2)$ intermolecular charge-transfer complexes (Table 7) where the decreases in ΔE_{bind} due to the ZPVE corrections are significant.

Results and Discussion

1. S_4, Se_4, and Te_4 Clusters. *S_4.* The S_4 cluster has been examined with many theoretical methods, and thus, a first step in the present study involved BLYP predictions on the S_4 species to determine the suitability of DFT in describing the X_4 potential energy surfaces. According to earlier works, HF[2,3] and CISD[2] methods predicted the global minimum to be the puckered ring structure. At multireference levels,[2,4] the global minimum was the open C_{2v} cis structure, with nonbonded terminal atoms. The closest critical point to the open C_{2v} cis minimum is the D_{2h} rectangular configuration **II**, which at the MR-CISD[2] level appears to be the transition state and is 1.0−2.3 kcal/mol higher than the open C_{2v} cis structure. Some correlated ab initio methods (MP2[3], MP4[3], QCISD(T))[5] and LDFT[6a] predict the rectangular species to be the global minimum rather than a transition state.

The geometries and relative energies of S_4 predicted with the BLYP/CEP-121(BPF) and BLYP/6-31G(BPF) methods are in good agreement with the earlier multireference results.[2,4] The open C_{2v} cis form is predicted to be the global minimum and the D_{2h} rectangular species corresponds to the transition state for the C_{2v} cis to C_{2v} cis degenerate interconversion, with a barrier of approximately 0.2 kcal/mol. A more localized terminal 3−4 bond length is predicted in comparison to multireference methods. In contrast to the multireference results,[2] the 1−2 and 3−4 bond lengths in the open C_{2v} cis structure are very slightly shorter (by 0.001 to 0.002 Å) than in the free S_2 molecule. The D_{2h} rectangular form shows a similar decrease in bond lengths relative to the free diatomic molecule. In general, the predictions of the open C_{2v} cis and D_{2h} rectangular systems from the BLYP methods are closer to each other in energies and geometries than in the earlier ab initio results.[2,5] The binding energies from BLYP for the open C_{2v} cis $S_2\cdots S_2$ structure are −17.7 kcal/mol with the 6-31G(BPF) and −16.5 kcal/mol with the CEP-121G(BPF) set. Since the predictions for S_4 depend strongly on the basis sets used, more reliable BLYP predictions on the open C_{2v} cis and D_{2h} rectangular configurations were made with the larger 6-311G(2df), 6-311+G(2df), and 6−311(3df) basis sets. Figure 3 illustrates the predicted geometries and the barrier height along with the QCISD(T)/6-311G(d) values.[5] With the all-electron triply split valence basis sets, the 1−2 and 3−4 bond lengths in the open C_{2v} cis structure are somewhat longer than in free S_2. The barrier for the C_{2v} cis to C_{2v} cis interconversion increases to 0.8 kcal/mol. The binding energy of the open C_{2v} cis structure increases to −20.3 kcal/mol with the 6-311(2df) and to −21.3 kcal/mol with the larger 6-311(3df) basis sets. In general, the differences in geometries and energies between the open C_{2v} cis and D_{2h} rectangular forms increases with larger basis sets and the open C_{2v} cis isomer of S_4 adopts a structure reminiscent of butadiene. These results are in very good agreement with the most accurate of the earlier conventional ab initio results[2,4,5] lending credence to our further research on the other chalcogens.

Se_4. Predictions for Se_4 are presented in Table 2. Very similar trends were obtained with the all-electron 6-311+G(2df) basis set and with LanL2DZ(BPF) core potential and basis set. The closed cis structure (trapezoidal four-membered ring) was found to be the global minimum, the C_{2h} trans structure is the closest isomer in energy, and the puckered ring is the highest. The 1−2 and 3−4 distances in the closed cis structure predicted with

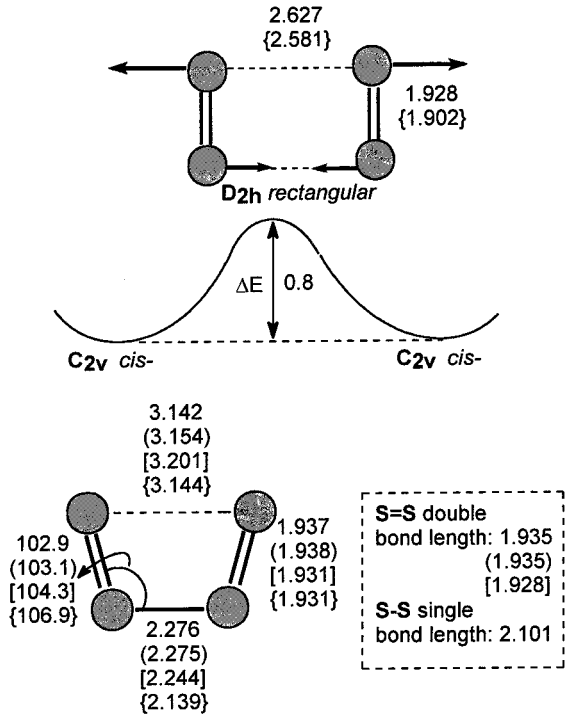

Figure 3. Predicted geometries (in Å and deg) for the C_{2v} cis minimum and the D_{2h} *rectangular* transition structure of the S_4 cluster. Theoretical methods were BLYP with the 6-311G(2df), 6-311+(2df) (values in parentheses), and 6-311G(3df) [square brackets] basis sets. Values in {curly brackets} are QCISD(T)/6−311(d) results from ref 5. The barrier height is in kcal/mol.

TABLE 2: Relative Energies ΔE_t (kcal/mol) and Bond Lengths and Angles (in Å and deg) for Se_4 Isomers[a]

basis sets/properties	cis	trans	branched ring	puckered ring
		ΔE_t		
6-311+G(2df)	0.0	6.1	13.7	17.9
LanL2DZ(BPF)	0.0	6.4	14.7	18.2
		Geometries		
6-311+G(2df)				
r_{12}	2.213	2.224	2.421	2.451
r_{23}	2.878	2.475	2.542	3.301
r_{14}	2.898			
r_{34}			2.225	
α	89.7	109.9	121.0	131.1
LanL2DZ(BPF)				
r_{12}	2.236	2.267	2.450	2.477
r_{23}	2.905	2.505	2.571	3.333
r_{14}	2.905			
r_{34}			2.245	
α	90.0	109.8	121.2	130.8

[a] All the predictions are from DFT with the BLYP functional. See Figure 1 for the atom numbering scheme.

the 6-311+G(2df) and LanL2DZ(BPF) basis sets decrease slightly compared to the free Se_2 molecule by 0.007 and 0.011 Å, respectively.

A difference between the all-electron triple-ζ plus polarization and core potential double-ζ basis set appears in the prediction of the symmetry of the closed ring structure, the global minimum of Se_4. The LanL2DZ(BPF) basis set predicts the D_{2h} rectangular form to be the global minimum. The C_{2v} cis species does not appear to be a critical point on the Se_4 potential energy surface with this basis set and collapses to the D_{2h} rectangular form during geometry optimization. In contrast, the larger 6-311+G-(2df) basis set qualitatively reflects the terrain near the global minimum on the X_4 potential energy surface expected on the basis of the S_4 results: the D_{2h} rectangular form is predicted to

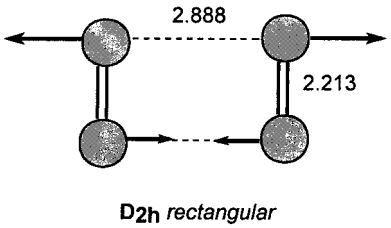

Figure 4. Distances (in Å) and transition state vector for the D_{2h} *rectangular* transition structure of Se_4 with the BLYP/6-311+G(2df) method.

be a transition state for the C_{2v} cis to C_{2v} cis rearrangement. The geometry and the transition vector of the D_{2h} rectangular configuration are depicted in Figure 4. Geometry optimization along the direction of the transition vector[23] leads to the C_{2v} structure. The potential energy surface in this region is very, very flat; the total energy decreases by only 0.2×10^{-7} hartree during optimization. Thus, it was impossible to reach a critical point, and consequently the closed C_{2v} cis configuration obtained cannot be unambiguously identified as a true minimum.

In summary, the barrier to the C_{2v} cis to C_{2v} cis rearrangement almost disappears on the potential energy surface of Se_4. Unlike the open C_{2v} cis form of S_4, the closed C_{2v} cis structure of Se_4 is extremely close to the D_{2h} rectangular configuration and has the same shorter 1−2 and 3−4 bonds compared to free diatomic molecules. Thus, the model of the binding arising through delocalization of the high-lying occupied π^*-antibonding orbitals of the X_2 subunits[2] can be applied to the Se_4 clusters. The increasing delocalization of the bond lengths in the series **I**−**V** of the Se_4 isomers leads to a decrease in their relative stability. Figure 5 shows the molecular orbital (MO) interaction diagram for the closed C_{2v} cis and the trans isomers of $(Se_2)(Se_2)$. The orbital energies of the a_u and a_g occupied MO of the C_{2h} trans structure with an "end to end" orientation of the Se_2 moieties decrease and the b_u occupied MO increases in energy on going to the closed C_{2v} cis isomer with a "face to face" orientation of the diatomics (b_1, a_1, and b_2 MO in C_{2v} symmetry, respectively). The total effect is a stabilization of the closed C_{2v} cis structure compared to the C_{2h} trans form. The predicted binding energies in the closed C_{2v} cis isomer are −18.5 kcal/mol with the LanL2DZ(BPF) and −21.3 kcal/mol with the 6-311+G(BPF) basis sets. The C_{2h} trans form is ca. 6 kcal/mol less stable. Electron density transfer from the π^*-antibonding portions of the b_1 and a_1 molecular orbitals leads to a decrease in the 1−2 and 3−4 distances in the closed C_{2v} cis isomer. The "end to middle" orientation of the diatomics in the branched ring is less effective in terms of orbital interactions than the cis and trans geometries. The energetically highest puckered ring isomer with a "middle to middle" orientation of the diatomics has all bond lengths equal and consequently cannot be viewed reasonably as an $(X_2)\cdots(X_2)$ interacting system at all. The puckered ring could be considered an analogue of the metastable O_4 ring[7] or of cyclobutadiene.

A comparison of the Mulliken overlap populations of the 2−3 and 1−4 interactions in the closed C_{2v} cis isomer of Se_4 and the open C_{2v} cis isomer of S_4 from BLYP/6-311+G(2df) method also revealed a difference between these two species. For S_4, the overlap population for the 2−3 interaction is 0.13 on the same order as a S−S single bond value (0.18 in the HS−SH molecule). The significantly smaller overlap population of 0.05 between the 1, 4 terminal S atoms corresponds to a weak stabilizing interaction rather than a chemical bond. In contrast, the overlap populations between the 2, 3 and 1, 4 atoms of 0.110 and 0.107 in the closed C_{2v} cis isomer of Se_4 are nearly equal and may be attributed to chemical bonding.

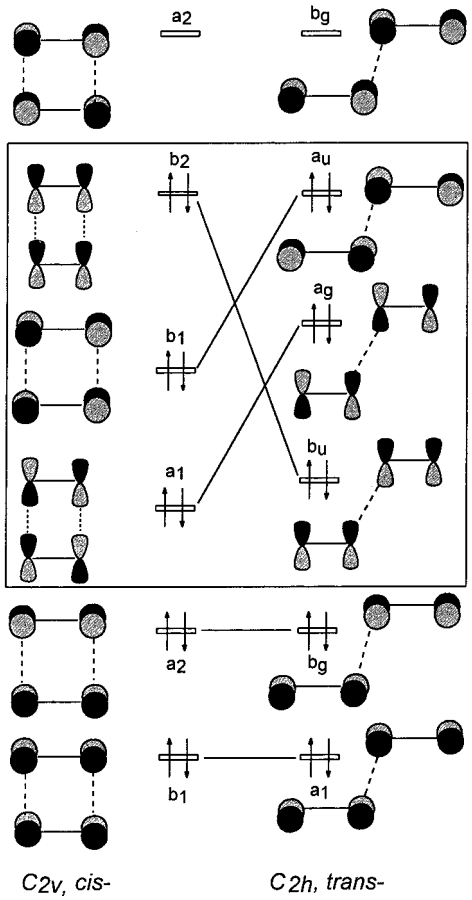

Figure 5. Orbital interaction diagram illustrating the stabilization of the C_{2v} cis isomer relative to the C_{2h} trans isomer of Se_4.

It has been shown for S_4[2] that the lowest triplet electron state isomers lie ca. 8 kcal/mol above the C_{2v} cis singlet. Given the increasing flatness of the potential energy surfaces of Se_4, there may be low-lying triplet states of the Se_4 clusters. With the LanL2DZ(BPF) basis set, the triplet isomers of Se_4 are predicted to lie only 3−5 kcal/mol higher than their singlet analogues. The larger all-electron basis set does not change these results significantly; with 6-311+G(2df) the C_{2h} trans- triplet isomer is 3.8 kcal/mol higher than the corresponding singlet species.

Te_4. The potential energy surfaces of S_4 and Se_4 are very flat with respect to variation of the distance or the angular orientation between the two interacting diatomic moieties in the region of the global minima. The flatness of these potential energy surfaces increases on going from S_4 to Se_4. Extrapolation to Te_4 would imply that the potential energy surface near the global minimum is a single potential well. These results are presented in Table 3. The pure BLYP functional predicts the same energetic ordering of the isomers for Te_4 as for the S_4 and Se_4 clusters. The hybrid B3LYP functional overestimates the relative stability of the puckered ring due to the inclusion of the HF exchange component into the exchange potential (recall Theoretical Details). It is predicted to be the closest in energy to the closed C_{2v} cis structure. However, both functionals and all basis sets predict the closed C_{2v} cis isomer to be the global minimum, with shorter 1−2 and 3−4 bonds relative to the lengths in free Te_2. The geometry of the closed C_{2v} cis structure is very close to the D_{2h} rectangular form, with the difference in lengths between the 2−3 and 1−4 bonds of 0.001 (HD basis set) to 0.029 Å from LanL2DZ(BPF). The BLYP functional with all basis sets employed predicts the branched ring and puckered ring isomers of Te_4 to be almost degenerate. Interestingly, the

TABLE 3: Relative Energies ΔE_t (kcal/mol) and Bond Lengths and Angles (in Å and deg) for theTe_4 Isomers[a]

properties/methods	cis	trans	branched ring	puckered ring
		ΔE_t		
BLYP/				
HD	0.0	5.3	9.2	9.2
LanL2DZ(BPF)	0.0	5.4	9.5	10.3
CEP-31G(BPF)	0.0	5.0	8.1	9.2
		Geometries		
BLYP/HD				
r_{12}	2.651	2.682	2.859	2.879
r_{23}	3.310	2.902	2.972	3.871
r_{14}	3.311			
r_{34}			2.665	
α		108.4	120.0	130.4
BLYP/LanL2DZ(BPF)				
r_{12}	2.609	2.642	2.823	2.847
r_{23}	3.260	2.865	2.935	3.817
r_{14}	3.289			
r_{34}			2.625	
α		108.6	120.6	129.2
BLYP/CEP-31G(BDF)				
r_{12}	2.647	2.680	2.857	2.882
r_{23}	3.293	2.902	2.969	3.862
r_{14}	3.295			
r_{34}			2.664	
α		108.7	121.4	128.9

[a] All the predictions are from DFT methods. See Figure 1 for the atom numbering scheme.

energies of interaction with BLYP between two Te_2 moieties in the closed C_{2v} cis form are essentially the same as for the S_4 and Se_4 clusters. The predicted binding energies are −17.3, −18.2, and −20.3 kcal/mol with the CEP-31(BPF), LanL2DZ-(BPF), and HD basis sets, respectively. The relative stabilities of the C_{2h} trans isomers also do not change on going from sulfur to tellurium. A stabilization of the branched ring and puckered ring isomers on going down the column may be explained in chemical terms by the increasing ability of the heavier elements to adopt higher coordination numbers.

For Te_4, the isomers on the lowest triplet state surface are even closer in energy to their singlet state analogues than in the case of the Se_4 cluster but all still lie higher in energy than the singlets. The BLYP/LanL2DZ(BPF) method predicts that the triplet isomers **I**, **III**, **IV**, and **V** are 5.2, 1.3, 2.6, and 0.4 kcal/mol higher than their closed-shell singlet analogues, respectively. It should be noted that the puckered ring isomer of Te_4 in its triplet electronic state collapses to a planar rhombus.

The results obtained for Te_4 clusters with DFT are in agreement with earlier theoretical investigations[11a] of the 1,2,3,5-ditelluradiazolyl species which contains a Te_4 fragment. The structure of the most stable isomer predicted with HF/LanL1DZ-(d) is depicted in Figure 6. The Te_4 fragment in the $[Te_2N_2-CH]_2$ dimer which consists of two weakly interacting units has the same closed C_{2v} cis structure as the most stable isomer of Te_4.

Harmonic Vibrational Frequencies. As is usually observed, the harmonic vibrational frequencies for all systems evaluated with DFT are smaller than those predicted with conventional ab initio methods and also smaller than the experimental fundamental values. However, general trends still may be obtained from the DFT level vibrational frequencies. The question of greatest interest concerns the structures of the two isomers whose IR and electronic absorption bands were observed for both the Se_4 and the Te_4 clusters.[1] For Se_4, one isomer is characterized by an IR band at 345 cm^{-1} while the other isomer has a band at 370 cm^{-1}. For the Te_4 isomers, IR

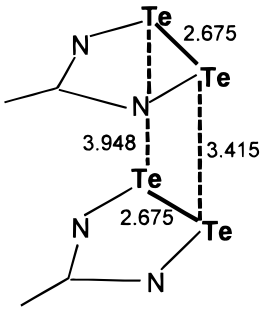

Figure 6. Selected geometrical parameters (in Å) for the most stable isomer of the ditelluradiazolyl dimer with HF/LanL1DZ(d) method from ref 11a. The Te_4 fragment is highlighted.

TABLE 4: BLYP Predictions of Selected Harmonic Vibrational Frequencies ω (cm^{-1}), with Their IR Intensities (km/mol) in Parentheses, and Force Constants f (mDyne/Å) for the Isomers I, III, IV, and V of S_4

	6-31G(BPF)	CEP-121(BPF)	6-311+G(2df)
	I, cis		
ω_1 sym stretch	650 (0)	644 (0)	647 (3)
ω_2 asym stretch	620 (94)	614 (31)	619 (101)
f_1	7.8	8.0	7.9
f_2	7.1	7.2	7.2
	III, trans		
ω_1 sym stretch	610 (0)	603 (0)	
ω_2 asym stretch	602 (130)	594 (138)	
f_1	6.8	7.0	
f_2	6.6	6.6	
	IV, branched ring		
ω_1 exo stretch	626 (118)	619 (128)	
ω_2 basal stretch	491 (8)	491 (9)	
f_1	7.2	7.4	
f_2	4.5	4.5	
	V, puckered ring		
ω_1 ring stretch	465 (0)	466 (0)	
f_1	4.1	4.1	

bands at 224 cm^{-1} and 243 cm^{-1} were observed. By analogy with the theoretical predictions of the vibrational frequencies for S_4[2], the lower IR band was assigned to the exocyclic X═X stretching vibration in the branched ring isomer and the other to the antisymmetric X═X stretching frequency in the cis isomer. Thus, the spectroscopically observed isomers of S_4, Se_4, and Te_4 previously have been assigned to the branched ring and C_{2v} cis structures.[1] Selected vibrational frequencies along with the IR intensities and force constants from the DFT approaches for the isomers **I**−**V** of S_4, Se_4, and Te_4 are collected in Tables 4−6. The highest vibrational frequencies are assigned to the stretching modes of the X−X bonds with considerable double bond character, i.e., the 1−2 and 3−4 bonds of the cis and trans isomers, and the 3−4 exocyclic and 1−2 basal bonds of the branched ring isomers. From the vibrational frequencies reported in Tables 4−6, the IR active modes are the asymmetric stretches for the C_{2v} cis and the C_{2h} trans structures and the exocyclic stretch of the terminal X═X bond in the branched ring structure. All DFT methods predict the same trend: the asymmetric stretch of the C_{2v} cis form and exocyclic stretch of the branched ring have nearly the same values. The asymmetric stretch in the C_{2h} trans structure is ca. 10 cm^{-1} lower in energy. The predicted IR active vibrational frequencies of the C_{2v} cis and branched ring structures indicate that these species are almost indistinguishable by IR spectroscopy. Tentatively, the highest IR band may be assigned to the cis and branched ring isomers of Se_4 and Te_4. The second IR band of lower energy then may be assigned to the trans isomers.

TABLE 5: BLYP Predictions of Selected Harmonic Vibrational Frequencies ω (cm^{-1}), with IR Intensities (km/mol) in Parentheses, and Force Constants f (mDyne/Å) for the Isomers I, III, IV, and V of Se_4

	6-311+G(2df)	LanL2DZ(BPF)
	I, cis	
ω_1 sym stretch	360[a] (0)	354 (0)
ω_2 asym stretch	342[a] (24)	336 (31)
f_1	6.1[a]	5.9
f_2	5.5[a]	5.3
	III, trans	
ω_1 sym stretch	327 (0)	326 (0)
ω_2 asym stretch	325 (47)	323 (42)
f_1	5.0	5.0
f_2	5.0	4.9
	IV, branched ring	
ω_1 exo stretch	326 (45)	337 (43)
ω_2 basal stretch	278 (3)	273 (3)
f_1	5.3	5.3
f_2	3.6	3.5
	V, puckered ring	
ω_1 ring stretch	267 (0)	262 (0)
f_1	3.3	3.2

[a] These values correspond to the D_{2h} rectangular structure **II** which is very close in energy and geometry to the cis structure **I**.

TABLE 6: BLYP Predictions of Selected Harmonic Vibrational Frequencies ω (cm^{-1}), with IR Intensities (km/mol) in Parentheses, and Force Constants f (mDyne/Å) for the Isomers I, III, IV, and V of Te_4

	HD	LanL2DZ(BPF)	CEP-31(BPF)
	I, cis		
ω_1 sym stretch	231 (0)	234 (0)	226 (0)
ω_2 asym stretch	222 (14)	224 (15)	217 (15)
f_1	4.1	4.2	3.9
f_2	3.8	3.8	3.6
	III, trans		
ω_1 sym stretch	212 (0)	216 (0)	210 (0)
ω_2 asym stretch	212 (14)	215 (22)	209 (22)
f_1	3.4	3.6	3.4
f_2	3.4	3.5	3.3
	IV, branched ring		
ω_1 exo stretch	230 (25)	224 (25)	217 (26)
ω_2 basal stretch	187 (1)	185 (2)	183 (1)
f_1	3.7	3.8	3.6
f_2	2.7	2.6	2.6
	V, puckered ring		
ω_1 ring stretch	182 (0)	179 (0)	176 (0)
f_1	2.5	2.4	2.4

Some useful information on the double bond character in the X_4 isomers can be obtained by comparing their vibrational frequencies and force constants in Tables 4−6 with the vibrational frequencies and force constants of the corresponding diatomic molecules (Table 1). The predicted vibrational frequencies and force constants for the symmetric stretches of the 1−2 and 3−4 bonds in the C_{2v} cis isomers of Se_4 and Te_4 are larger than in the comparable diatomic molecules. The increases in these values mirror the decreasing 1−2 and 3−4 bond lengths compared to the free diatomic molecules values, in accord with Badger's rules.[25] In summary, the vibrational frequencies and the force constants as well as the geometries and the overlap populations predicted with the BLYP functional highlight the different nature of binding for the open C_{2v} cis isomer of S_4 and the closed C_{2v} cis isomers of the Se_4 and Te_4 clusters.

2. (Se_2)(O_2) and (Te_2)(O_2) Intermolecular Charge-Transfer Complexes. The interactions of the Se_2 and Te_2 diatomic molecules with molecular oxygen lead to weakly bound closed-shell singlet electronic state intermolecular complexes with the

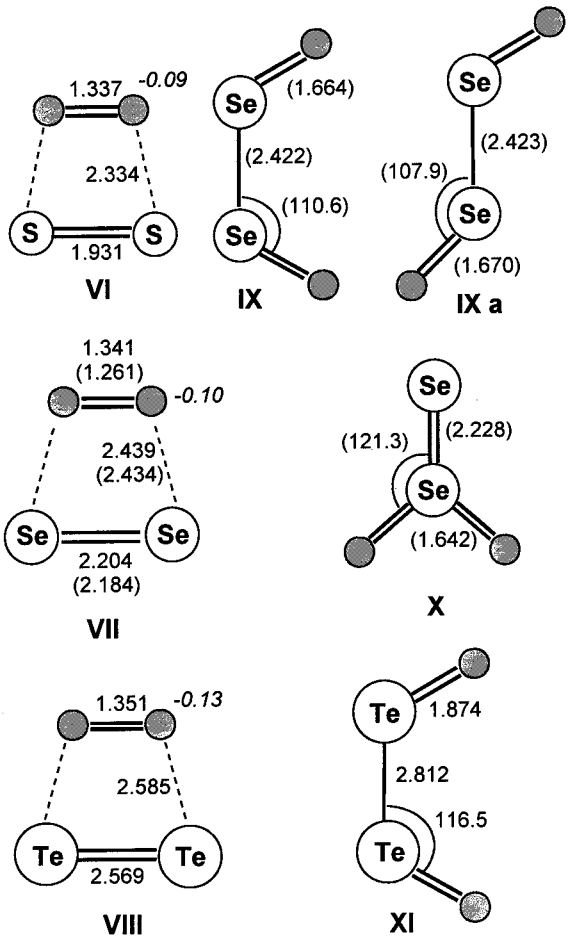

Figure 7. Predicted geometries (in Å and deg) and selected Mulliken atomic charges (*italics*) for **VI**−**XI** with the basis sets 6-311+G(2df) (values in parentheses) and LanL2DZ with BPF on the chalcogen atoms.

C_{2v} cis structures **VII** and **VIII**. These are depicted in Figure 7 along with the other isomers. The geometry and energetics of the sulfur analogue **VI** were predicted for comparison. Other possible orientations of two interacting O_2 and S_2 molecules in various electronic states have been studied[12] theoretically but only the closed-shell singlet C_{2v} cis configuration with parallel orientation of the diatomic moieties was found to be stable. We propose herein that similar preferences will exist for the $(Se_2)(O_2)$ and $(Te_2)(O_2)$ complexes. Given that the $(S_2)(O_2)$ and $(Se_2)(O_2)$ complexes demonstrated much the same properties in spectroscopic experiments, similar spectral changes and energetics might be extrapolated to the $(Te_2)(O_2)$ charge-transfer complex.

Two interacting diatomics, X_2 (X = S, Se, Te) and O_2, may be described by the same qualitative molecular orbital diagram depicted in Figure 5 for the C_{2v} cis isomer of Se_4. Thus, bonding through delocalization of electron density from the π*-antibonding orbitals which stabilizes the "face to face" orientation of the diatomic moieties occurs. Given the considerable difference in electronegativities of the interacting diatomic molecules when O_2 is one partner stabilization due to delocalization is expected to be smaller on the basis of the orbital interaction diagram than in the case of the clusters. There is only a small charge transfer from the X_2 to O_2 moiety.

Table 7 presents the BLYP results for **VI**, **VII**, and **VIII** with the LanL2DZ basis set with BPF on the X_2 moieties. All complexes show very similar features: the shortening of the X−X bond lengths and the lengthening of the O−O bonds compared to their free diatomics values, small blue shifts in the X−X harmonic vibrational frequencies, and red shifts in the O−O harmonic vibrational frequencies. In general, these results are in accord with the data from the earlier spectroscopic study.[12] Unlike the IR experiments,[12] which measured very similar spectra for both **VI** and **VII**, the DFT approach predicts a decrease in the blue shifts and an increase in the red shifts on going from $(S_2)(O_2)$ to $(Te_2)(O_2)$. The binding energies and Mulliken charges on the oxygen atoms increase down this column of the periodic table. The same trends were predicted theoretically for charge-transfer complexes between ethylene and diatomic halogen molecules on proceeding from F_2 to I_2.[13a]

TABLE 7: Binding Energies ΔE_{bind} (kcal/mol), with the ZPVE Corrected Values in Parentheses (kcal/mol), Red Shifts for the O−O Stretch Vibrational Mode $\Delta\nu_{O-O}$ and Blue Shifts for the X−X Stretch Vibrational Mode $\Delta\nu_{X-X}$ (cm^{-1}), Lengthening of the O−O Bonds Δl_{O-O} (Å) and Shortening of the X−X Bonds Δl_{X-X} (Å) for the $(S_2)(O_2)$, $(Se_2)(O_2)$, and $(Te_2)(O_2)$ Complexes[a]

complex	ΔE_{bind}	$\Delta\nu_{O-O}$	$\Delta\nu_{X-X}$	Δl_{O-O}	Δl_{X-X}
$(S_2)(O_2)$	−3.1 (−1.6)	179	23	0.037	0.036
$(Se_2)(O_2)$	−4.1 (−2.8)	192	15	0.041	0.043
$(Te_2)(O_2)$	−4.4 (−3.3)	219	13	0.051	0.049

[a] All the predictions are from the BLYP/LanL2DZ(BPF) method.

To place these $(X_2)(O_2)$ charge-transfer complexes in the context of the full potential energy surfaces of the X_2O_2 systems, several plausible isomers of the Se_2O_2 and Te_2O_2 systems also were examined. Earlier research[27a] on the Se_2O_2 systems with the B3LYP functional predicted that the open cis and trans OSeSeO structures are nearly degenerate and, likely, are the lowest minima. Extrapolation suggests that similar isomers will be the most stable for the Te_2O_2 system. For the related S_2O_2 system, the open cis OSSO structure was determined as the most stable isomer in a microwave spectroscopic experiment.[26] However, the CCD/TZ2P method predicted[27b] that the open cis OSSO structure is only a local minimum on the potential energy surface of S_2O_2. The global minimum was predicted to have a thio S=SO_2 structure. A similar Se=SeO_2 isomer might compete energetically with the cis and trans isomers.

For Se_2O_2, BLYP/6-311+G(2df) predicted that the cis isomer **IX** is 31.3 kcal/mol more stable than the Se=SeO_2 species **VII**. The trans **IXa** and the cis **IX** are almost degenerate with a chemically insignificant energetic preference for the cis form in good accord with the earlier B3LYP predictions.[27a] **X** is predicted to be 20.1 kcal/mol less stable than **XI**. For the Te_2O_2, complex **VIII** is 25.7 kcal/mol higher than the cis **XI** at the BLYP/LanL2DZ(BPF) level. In summary, the intermolecular weakly bound charge-transfer $(X_2)(O_2)$ complexes may be considered as metastable systems corresponding to higher lying local minima on the X_2O_2 potential energy surfaces.

3. $(Se_2)(S_2)$, $(Te_2)(S_2)$, and $(Se_2)(Te_2)$ Mixed Compounds. Chalcogens are elementally similar and, thus, the structures, bond lengths, and binding energies in the mixed compounds composed from homo- and hetronuclear diatomic moieties should resemble those in the clusters considered above. However, due to the differences in the electronegativities of the tellurium and sulfur atoms, a small charge transfer from the Te_2 to the S_2 diatomic fragments in the $(Te_2)(S_2)$ system would be expected. The geometrical parameters and energetics predicted with the BLYP/LanL2DZ(BPF) method are given in Figures 8, 9, and 10 for the Se_2S_2, Te_2S_2, and Se_2Te_2 systems, respectively. For all of the "mixed" compounds considered, the closed-shell singlet cis structures, with a nonparallel orientation of the interacting diatomic moieties **XII** (**XV**), **XVII**, and **XXIV** were predicted to be the global mimima. Predicted binding

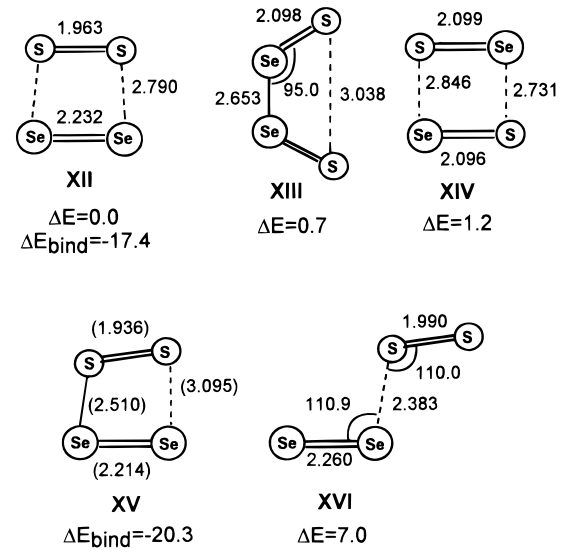

Figure 8. Predicted geometries (in Å and deg), relative energies ΔE (kcal/mol), and binding energies ΔE_{bind} (kcal/mol) for the isomers **XII**−**XVI** of Se_2S_2 with the LanL2DZ(BPF) and 6-311+G(2df) (values in parentheses) basis sets.

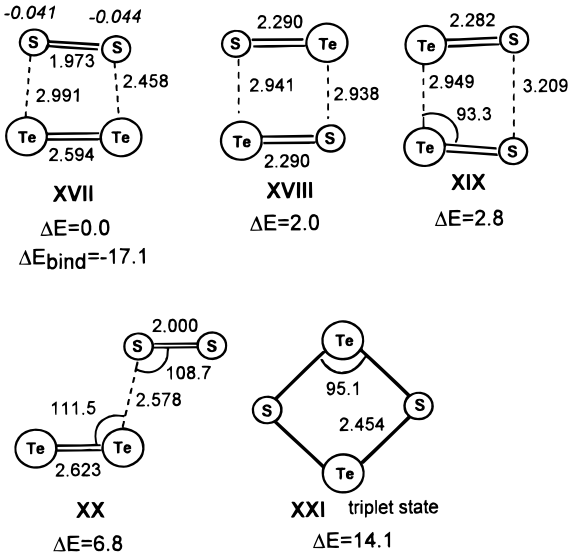

Figure 9. Predicted geometries (in Å and deg), relative energies ΔE (kcal/mol), and binding energies ΔE_{bind} (kcal/mol) for the isomers **XVII**−**XXI** of Te_2S_2 with the LanL2DZ(BPF) basis set.

energies are of the same order of magnitude as in the X_4 clusters (ca. −17 to −19 kcal/mol). For the Se_2S_2 cis structures (Figure 8), the exact angular orientation of the Se_2 and S_2 diatomic molecules depends on the basis set employed. The LanL2DZ-(BPF) basis set predicts the C_{2v} structure **XII** with a parallel orientation of diatomic molecules similar to the rectangular isomer of the Se_4 cluster. The larger 6-311+G(2df) basis set predicts a C_s structure **XV** with a nonparallel orientation of the diatomic moieties in Se_2S_2.

The (SeS)(SeS) and (TeS)(TeS) C_s cis isomers **XIV** and **XVII** were found to be very close in energy to the $(Se_2)(S_2)$ and (Te_2)-(S_2) cis forms, with a very small preference in energy for the isomers viewed as constructed from the homonuclear diatomic molecules. For the Te_2Se_2 system, the $(Te_2)(Se_2)$ cis structure **XXII** was predicted to be a transition state which is 5.5 kcal/mol higher than the minimum with nonplanar structure **XXIII**. The most stable $(Te_2)(Se_2)$ isomer was predicted to have the trans structure **XXVIII**. For all systems considered, the trans

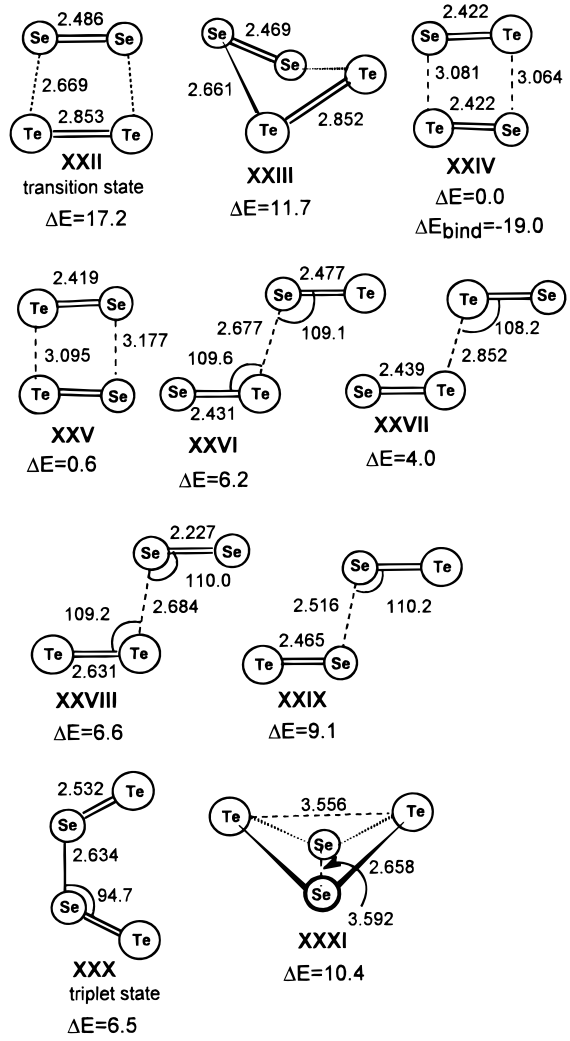

Figure 10. Predicted geometries (in Å and deg), relative energies ΔE (kcal/mol), and binding energies ΔE_{bind} (kcal/mol) for the isomers **XXII**−**XXXI** of the Te_2Se_2 species.

isomers lie ca. 4−7 kcal/mol higher than their cis counterparts which is similar to the behavior observed for the X_4 clusters.

The Se−Se and S−S bond lengths in **XII** are 0.015 and 0.004 Å shorter after formation of the complex compared to the free Se_2 and S_2 molecules, respectively. The S−S bond length in **XV** has the same value as in the free S_2 molecule, and the Se−Se bond is shorter by 0.005 Å compared to the free Se_2 diatomic molecule. Due to the increasing difference between the electronegativities of the diatomic chalcogens in Te_2S_2 compared to Se_2S_2, the C_s cis structure of Te_2S_2 demonstrates some features of the charge-transfer complexes with oxygen which were discussed above. The bond length of S_2 with the greater electronegativity is longer and the bond length of the Te_2 subunit with the smaller electronegativity which is shorter relative to the free diatomic bond lengths. The Mulliken charges on the S atoms in **XV** are small but negative. Therefore, a small electron density transfer from the π^*-antibonding orbital of the Te_2 to the π^*-antibonding orbital of the S_2 moiety has occurred. For the (SeTe)(SeTe) isomers **XXIV** and **XXV**, the Se═Te bond lengths are shorter by 0.007 and 0.01 Å, respectively, than those predicted for the free SeTe molecule.

All triplet isomers of the mixed compounds were predicted to be slightly higher in energy than their singlet state analogues. The triplet isomers of **XII** and **XVI** lie 5.0 and 4.8 kcal/mol higher than these singlets, respectively. For Te_2Se_2, the most

stable triplet isomer was predicted to have a planar cis structure **XXX** with Se═Te terminal double bonds.

Summary and Conclusions

Two triplet state diatomic molecules X_2 (X = Se, Te) containing formally double bonds can interact to form closed-shell singlet state tetra-atomic clusters. There are four energetically favorable configurations: "face to face", "head to head", "head to middle", and "middle to middle". The corresponding isomers ordered according to their relative stabilities are: closed C_{2v} cis, C_{2h} trans, C_s branched ring, and D_{2d} puckered ring. The closed C_{2v} cis structure is stabilized by a delocalization of the electron density in the high-lying occupied orbitals which are π*-antibonding for the interacting diatomic fragments but are π- or σ-bonding for the two "new" bonds formed upon interaction. The predicted binding energies are ca. −18 kcal/mol with ECP basis sets and ca. −21 kcal/mol with all-electron basis sets. For the C_{2h} trans isomers where electron density from π*-antibonding orbitals on the fragments migrates to only one "new" bond, the stabilization is ca. −12 or 6 kcal/mol less than in the C_{2v} cis form. The C_s branched ring and the D_{2d} puckered ring with less delocalization are even less stable. Thus, the closed C_{2v} cis isomers are the global minima on the potential energy surfaces of the X_4 clusters.

As a result of the withdrawal of electron density from the occupied π*-antibonding orbitals the X═X bonds are shorter than in the free diatomic molecules. The trapezoidal closed C_{2v} cis structures are very close in geometry to the D_{2h} rectangular configuration; that is, the "double" bonds of the diatomic fragments are nearly parallel and the two parallel "new" bonds have almost equal lengths. Thus, the closed C_{2v} cis structures of Se_4 and Te_4 are different from the open C_{2v} cis structure of S_4. S_4 has only a weak stabilizing interaction between the terminal sulfur atoms and thus, in general, is similar to the cis butadiene structure. Despite the different natures of binding, all tetra-atomic chalcogens have similar potential energy surfaces with the same energetic order of the local minima and a similar, complicated topology near the global minima. For S_4 and Se_4, these regions contain a double well potential which corresponds to the degenerate C_{2v} cis to C_{2v} cis rearrangement through the D_{2h} rectangular transition state. The very small barrier of 0.8 kcal/mol for S_4 becomes a chemically insignificant value for Se_4 and disappears for Te_4. Thus, for Te_4 there is a simple potential well with a very flat bottom.

Mixed $(X_2)(Y_2)$ and (XY)(YX) compounds (X, Y = S, Se, Te) have the same nature of binding as the Se_4 and Te_4 clusters. Consequently, the same closed C_{2v} cis structures are the most stable isomers. The isomers with homonuclear diatomic fragments were predicted to be very close in energy to the isomers from the heterodiatomic moieties. The stabilities of the species with heteronuclear diatomic molecules relative to the isomers from the homonuclear diatomic molecules increases with a decrease in the difference between the electronegativities of the chalcogen atoms; (TeS)(TeS) is less stable than $(Te_2)(S_2)$, but (TeSe)(TeSe) is more stable than the $(Te_2)(Se_2)$ system. This conclusion agrees with the experimental X-ray structure a for $Te_2(S_2PPH_2)_2$[30] which is shown in Figure 11. The observed geometry clearly indicates a S−Te−Te−S bonding arrangement. The alternative structure b with S−Te−S equal bonds is unobserved, although such a structure is typical for the $Co_2(S_2PPH_2)_2$ and $Au_2(S_2PPH_2)_2$ systems. In general, the relative stability of the mixed (XY)(YX) compounds increases slightly down the column of chalcogens in the periodic table.

The binding energies of the intermolecular $(Se_2)(O_2)$ and $(Te_2)(O_2)$ charge transfer complexes are only ca. −2 kcal/mol and ca. −3 kcal/mol, respectively. These complexes adopt the C_{2v} cis structure with a parallel orientation of the diatomic subunits. Given the greater difference between the electronegativities of the interacting diatomic moieties, delocalization of electron density from the π*-antibonding orbitals on the fragments is significantly smaller than in the cases of the clusters and mixed compounds. Thus, $(Se_2)(O_2)$ and $(Te_2)(O_2)$ correspond to higher lying local minima. Due to the transfer of electron density from Se_2 and Te_2 to the O_2 subunits, the bond lengths in the chalcogen diatomic moieties are shorter and the bond lengths in the O_2 moieties are longer relative to their free diatomic values. The small blue shifts of the chalcogen stretch and the red shifts of the O_2 stretch are in qualitative agreement with IR spectroscopic data. DFT predicts an increase in binding energies and in spectral shifts on proceeding down the column of the group 16 elements in the periodic table.

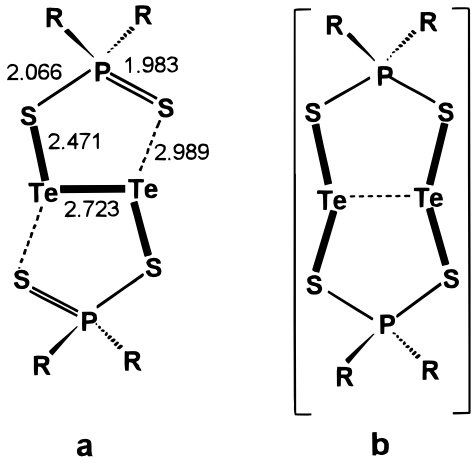

Figure 11. $Te_2(S_2PPh_2)_2$. Observed structure a with selected X-ray geometrical parameters (in Å) from ref 30 and hypothetical structure b. The S−Te−Te−S and S−Te−S linkages are highlighted.

The predicted structural trends may be applied to larger molecules containing these tetra-atomic fragments. Thus, the distortions in dithia-, diselena-, or ditelluradiazolyl dimers may be explained on the basis of nonparallel orientations of the X═X (X = chalcogen) bonds in the X_4 structural fragments. For mixed compounds of tellurium and selenium, a preference for isomers with Te−Se linkages is predicted. In contrast, for mixed compounds of selenium or tellurium with sulfur, an energetic preference for isomers with homonuclear bonding is anticipated.

Acknowledgment. Financial support of this research by the Natural Sciences and Engineering Research Council of Canada (NSERC) is gratefully acknowledged.

References and Notes

(1) Brabson, G. D.; Mielke, Z.; Andrews, L. *J. Phys. Chem.* **1991**, *95*, 79. (b) Hassanzadeh, P.; Andrews, L. *J. Phys. Chem.* **1992**, *96*, 6579. (c) Hassanzadeh, P.; Thompson, C. A.; Andrews, L. *J. Phys. Chem.* **1992**, *96*, 8246. (d) Brabson, G. D.; Anderson, L. *J. Chem. Phys.* **1992**, *96*, 9172. (e) Licovsky, G. *The Physics of Selenium and Tellurium*; Gerlach, E., Grosse, P., Eds.; Springer; Berlin, 1979; p 178. (f) Cordes, A. W.; Haddon, R. C.; Oakley, R. T. *The Chemistry of Inorganic Ring Systems*; Steudel, R., Ed.; Elsevier: Amsterdam, 1992; p 295. (g) Goodman, J.; Brus, L. E. *J. Chem. Phys.* **1977**, *67*, 4398. (h) Li, Z. Q.; Yu, J. Z.; Ohno, K.; Gu, B. L.; Czajka, R.; Kasuya, A.; Nishina, Y.; Kawazoe, Y. *Phys. Rev. B* **1995**, *52*, 1524. (i) Helm, H.; Walter, C. W. *J. Chem. Phys.* **1993**, *98*, 5444. (j) Hanold, K. A.; Continetti, R. E. *Chem. Phys.* **1998**, *239*, 493.

(2) Quelch, G.; Schaefer, H. F., III; Marsden, C. J. *J. Am. Chem. Soc.* **1990**, *112*, 8719.

(3) Raghavachari, K.; Rohlfing, C. M.; Binkley, J. S. *J. Chem. Phys.* **1990**, *93*, 5862.

(4) Von Niessen, W. *J. Chem. Phys.* **1991**, *95*, 8301.
(5) Abboud, J.-L. M.; Esseffar, M.; Herreros, M.; Mo, O.; Molina, M. T.; Notario, R.; Yanez, M. *J. Phys. Chem.* **1998**, *102*, 7996.
(6) Hohl, D.; Jones, R. O.; Car, R.; Parrinello, M. *J. Chem. Phys.* **1988**, *89*, 6823. (b) Hohl, D.; Jones, R. O.; Car, R.; Parrinello, M. *Chem. Phys. Lett.* **1987**, *139*, 540.
(7) Seidl, E. T.; Schaefer, H. F., III *J. Chem. Phys.* **1992**, *96*, 1176.
(8) Ahmed, F.; Nixon, E. R. *J. Mol. Spectrosc.* **1981**, *87*, 101. (b) *The Physics of Selenium and Tellurium*; Gerlach, E., Grosse, P., Eds.; Springer-Verlag: Berlin, Heidelberg, New York, 1979; p 267, 272. (c) Haiduc, I.; King, R. B.; Newton, M. G. *Chem. Rev.* **1994**, *94*, 301. (d) Beck, J. *Angew. Chem., Int. Ed. Engl.* **1994**, *33*, 163. (e) Lyne, P. L.; Mingos, D. M. P.; Ziegler, T. *J. Chem. Soc., Dalton Trans.* **1992**, 2745.
(9) Huber, K. P.; Herzberg, G. *Constants of Diatomic Molecules*; Van Nostrand Reinhold: New York, 1979. (b) Andrews, L.; Smardzewski, R. R. *J. Chem. Phys.* **1973**, *58*, 2258. (c) Pauling, L. *The nature of the chemical bond*; Cornell University Press: Ithaca, NY, 1960. (d) Lide, D. R. *Handbook of Chemistry and Physics*, 73rd ed.; CRC Press: Boca Raton, FL, 1992−1993. (e) Brabson, G. D.; Mielke, Z.; Andrews, L. *J. Phys. Chem.* **1991**, *95*, 79.
(10) Seidl, E.; Schaefer, H. F., III *J. Chem. Phys.* **1988**, *88*, 7043.
(11) Davis, W. M.; Goddard, J. D. *Can. J. Chem.* **1996**, *74*, 810. (b) Cordes, A. W.; Bryan, C. D.; Davis, W. M.; de Laat, R. H.; Glarum, S. H.; Goddard, J. D.; Haddon, R. C.; Hicks, R. G.; Kennepohl, D. K.; Oakley, R. T.; Scott, S. R.; Westwood, N. P. C. *J. Am. Chem. Soc.* **1993**, 7232.
(12) Brabson, G. D.; Citra, A.; Andrews, L.; Davy, R. D.; Neurock, M. *J. Am. Chem. Soc.* **1996**, *118*, 5469.
(13) Ruiz, E.; Salahub, D. R.; Velta, A. *J. Am. Chem. Soc.* **1995**, *117*, 1141. (b) Proynov, E. I.; Salahub, D. R. *Int. J. Quantum Chem., Symposium* **1995**, *29*, 61.
(14) Frisch, M. J.; Trucks, G. W.; Schlegel, H. B.; Scuseria, G. E.; Robb, M. A.; Cheeseman, J. R.; Zakrzewski, V. G.; Montgomery, J. A.; Stratmann, R. E.; Burant, J. C.; Dapprich, S.; Millam, J. M.; Daniels, A. D.; Kudin, K. N.; Strain, M. C.; Farkas, O.; Tomasi, J.; Barone, V.; Cossi, M.; Cammi, R.; Mennucci, B.; Pomelli, C.; Adamo, C.; Clifford, S.; Ochterski, J.; Petersson, G. A.; Ayala, P. Y.; Cui, Q.; Morokuma, K.; Malick, D. K.; Rabuck, A. D.; Raghavachari, K.; Foresman, J. B.; Cioslowski, J.; Ortiz, J. V.; Stefanov, B. B.; Liu, G.; Liashenko, A.; Piskorz, P.; Komaromi, I.; Gomperts, R.; Martin, R. L.; Fox, D. J.; Keith, T.; Al-Laham, M. A.; Peng, C. Y.; Nanayakkara, A.; Gonzalez, C.; Challacombe, M.; Gill, P. M. W.; Johnson, B. G.; Chen, W.; Wong, M. W.; Andres, J. L.; Head-Gordon, M.; Replogle, E. S.; Pople, J. A. *Gaussian98*; Gaussian, Inc.: Pittsburgh, PA, 1998.
(15) Becke, A. D. *Phys. Rev. A* **1988**, *38*, 3098.
(16) Becke, A. D. *J. Chem. Phys.* **1993**, *98*, 5648.
(17) Lee, C.; Yang, W.; Parr, R. G. *Phys. Rev. B* **1988**, *37*, 785. Miechlish, B.; Savin, A.; Stoll, H.; Preuss, H. *Chem. Phys. Lett.* **1989**, *157*, 200.
(18) Binning, R. C.; Curtiss, L. A. *J. Comput. Chem.* **1990**, *11*, 1206. Curtiss, L. A.; McGrath, M. P.; Blaudeau, J.-P.; Davis, N. E.; Binning, R. C.; Radom, L. *J. Chem. Phys.* **1995**, *103*, 6104. McGrath, M. P.; Radom, L. *J. Chem. Phys.* **1991**, *94*, 511. (b) Ditchfield, R.; Hehre, W. J.; Pople, J. A. *J. Chem. Phys.* **1971**, *54*, 724. Hehre, W. J.; Ditchfield, R.; Pople, J. A. *J. Chem. Phys.* **1972**, *56*, 2257. Hariharan, P. C.; Pople, J. A. *Mol. Phys.* **1974**, *27*, 209. Gordon, M. S. *Chem. Phys. Lett.* **1980**, 76, 163. Hariharan, P. C.; Pople, J. A. *Theor. Chim. Acta* **1973**, *28*, 213.
(19) Poirier, R.; Kari, R.; Csizmadia, I. G. *Handbook of Gaussian Basis Sets*; Elsevier: New York, 1985.
(20) Stevens, W. J.; Basch, H.; Krauss, M. *J. Chem. Phys.* **1984**, *81*, 6026. Stevens, W. J.; Krauss, M.; Basch, H.; Jasien, P. G. *Can. J. Chem.* **1992**, *70*, 612. Cundari, T. R.; Stevens, W. J. *J. Chem. Phys.* **1993**, *98*, 5555.
(21) Hay, P. J.; Wadt, W. R. *J. Chem. Phys.* **1985**, *82*, 270. Wadt, W. R.; Hay, P. J. *J. Chem. Phys.* **1985**, *82*, 284. Hay, P. J.; Wadt, W. R. *J. Chem. Phys.* **1985**, *82*, 299. (b) Dunning, T. H.; Hay, P. J. In *Modern Theoretical Chemistry*; Schaefer, H. F., Ed.; Plenum: New York, 1976; pp 1−28.
(22) Basch, H. *Chem. Phys. Lett.* **1989**, *157*, 129.
(23) Minyaev, R. M. *Int. J. Quantum Chem.* **1994**, *49*, 105.
(24) Goddard, J. D.; Chen, X.; Orlova, G. *J. Phys. Chem. A* **1999**, *103*, 4078.
(25) Badger, R. M. *J. Chem. Phys.* **1934**, *2*, 128; **1934**, *3*, 710.
(26) Lovas, F. J.; Tiemann, E.; Johnson, D. R. *J. Chem. Phys.* **1974**, *60*, 5005.
(27) Brabson, G. D.; Andrews, L.; Marsden, C. J. *J. Phys. Chem.* **1996**, *100*, 16487. (b) Marsden, C. J.; Smith, B. J. *Chem. Phys.* **1990**, *141*, 335.
(28) Smart, B. A.; Schiesser, C. H. *J. Comput. Chem.* **1995**, *16*, 1055.
(29) Jones, R. O.; Hohl, D. *J. Am. Chem. Soc.* **1990**, *112*, 2590.
(30) Newton, M. G.; King, R. B.; Haiduc, I.; Silvestru, A. *Inorg. Chem.* **1993**, *32*, 3795.